

# OPTIMIZATION OF A CITRUS CANOPY SHAKER HARVESTING SYSTEM: PROPERTIES AND MODELING OF TREE LIMBS

S. K. Gupta, R. Ehsani, N. H. Kim

**ABSTRACT.** *This article presents a part of the research work for the design and optimization of a fruit tree harvesting system using numerical methods. The analytical framework for the optimization is formulated based on a continuous canopy shaker that harvests citrus crops, primarily Valencia oranges (Citrus sinensis). Tree limbs are modeled analytically in the numerical based design optimization of a shaker that requires information regarding the limb configuration and properties. The objective of this study is to formulate a mathematical model to predict the configuration of primary limbs and to determine the properties of citrus wood. The tree limbs, thus proposed, are statistical prototypes or representations that account for the 5th, 25th, 50th, 75th, and 95th percentiles of actual tree limbs from random individual citrus trees. Polynomial response surface models were developed to predict sectional properties of the statistical model of the tree limbs. The distributions of the secondary branches and fruits were also predicted to model their effect on the dynamic response of the tree limbs. A three-point bending test, specific gravity test, moisture content test, and damping test were conducted on freshly cut samples of citrus wood. An elastic modulus of 8.5 GPa and modulus of rupture of 67.3 MPa were calculated from a load-deflection curve, and a density of  $1450.8 \text{ kg m}^{-3}$ , moisture content of 42%, and damping ratio of 10.78 were measured. Although the proposed methodology was developed for a canopy shaker, it could be easily implemented for other vibratory harvesters, such as limb shakers, foliage shakers, and over-the-row harvesters.*

**Keywords.** *Canopy shaker, Citrus, Dynamic simulation, Finite element methods, Harvester, Modeling, Optimization, Response surface.*

**M**echanical harvesting of tree crops is becoming increasingly important due to the cost of manual harvesting. Competitiveness in the global market demands efficient harvesting systems to reduce harvesting costs. Many mechanical harvesters for fruits and nuts have been developed over the past five decades, but few of them have been successfully adopted and commercialized (Futch et al., 2004). Many commercialized harvesters for fruits and nuts are designed to induce either free vibration or forced vibration to the trunk or tree limbs and canopy (Fridley et al., 1971; Peterson et al., 1972; Markwardt et al., 1964; Halderson, 1966). These vibrations are then transmitted throughout the tree, creating the forces necessary to cause fruit detachment. These harvesters are essentially comprised of two parts: the mechanical system that generates vibratory motions, and the mechanical interface that transmits vibrational energy to the tree. Examples of mechanical interfaces include movable tongs that grip the trunk or limbs and force them to vibrate, or a vibrating rod that impacts the tree limbs to

cause them to vibrate freely.

Most accomplishments in the design of vibratory harvesters have been achieved using heuristic methods (Fridley and Adrian, 1966). This involves designing the harvesting system using either a trial and error approach or an approach based on certain assumptions validated later by extensive field trials. However, field trials are usually very costly and time-consuming. Moreover, the specific problem areas are difficult to evaluate by experimental studies due to the high variability and randomness associated with the trees and their interaction with the harvester. While past field trials have provided a general understanding of the dynamic response of tree crops, the parameters necessary to design a harvester have not yet been formulated. The explanation for good harvesting yield under some conditions and excessive tree damage in other cases was found to be related to the tree structure and its interaction with the harvester (Fridley and Adrian, 1966). Extensive field trials would be required to formulate these interactions in order to find the optimum harvesting parameters; however, they would be prohibitively expensive and time-consuming.

An alternative approach for designing an efficient harvesting system is to use numerical methods (Archer, 1965; Hurty and Rubinstein, 1964). Experimentally verified numerical models allow a machine designer to economically iterate designs to select the optimal design. Finite elements (FE) methods are widely used numerical techniques in structural design. However, the application of these methods in the design of a harvesting system is limited because of the complicated and non-uniform nature of biological

---

Submitted for review in June 2014 as manuscript number MS 10818; approved for publication by the Machinery Systems Community of ASABE in June 2015.

The authors are **Susheel K. Gupta**, Graduate Student, and **Reza Ehsani, ASABE Member**, Associate Professor, Citrus Research and Education Center, University of Florida, Lake Alfred, Florida; **Nam-Ho Kim**, Associate Professor, Department of Mechanical and Aerospace Engineering, University of Florida, Gainesville, Florida. **Corresponding author:** Reza Ehsani, 700 Experiment Station Road, Lake Alfred, FL 33850; phone: 863-956-1151, ext. 1228; e-mail: ehsani@ufl.edu.

structures such as tree limbs. Moreover, the randomness in the spatial configuration of tree limbs and their interaction with a harvesting system makes the physical phenomenon very difficult to simulate using numerical methods. Some assumptions and generalizations should be made to efficiently approximate the physical models and their interactions. FE methods can be an economical way to optimize a harvesting system because of their capability to iterate a large number of designs in significantly less time as compared to building machines and testing them in the field.

In the past, analytical models have been developed for modeling tree crops and their interactions with various types of harvesting systems such as trunk shakers, limb shakers, canopy or foliage shakers, and over-the-row harvesters. The dynamic characteristics of the tree limb and fruit system were predicted using various numerical methods. Fridley and Yung (1975) used FE methods to model a whole tree, including the fruit-stem system. They developed three special FE models to mathematically describe a tree system and evaluated the natural frequencies, mode shapes, and dynamic internal stress of the complete tree structure for steady-state forced vibration. Rumsey (1967a) modeled the fruit-stem system as an elastic beam with a concentrated load at one end and studied the effect of inertial forces due to the mass of the fruits on the bending and shear of a tree limb modeled as a beam. Pestel and Leckie (1963) studied the vibration response of non-uniform beams using matrix methods. Later, the method of transfer matrices was applied by Rumsey (1967b) to solve the forced response of non-uniform beams using FE methods. Fridley and Lorenzen (1965) simulated tree shaking by modeling the limb as a four-cell cantilever beam. They used classical Euler-Bernoulli beam theory to formulate partial differential equations. The equations were solved using FE methods to predict the beam response when vibrated with constant force and varying frequency. Schuler and Bruhn (1973) applied Timoshenko beam theory with structural damping to formulate differential equations for the dynamic response of the limbs. They concluded that rotary inertia has very little effect on the beam response, while the presence of deflection due to shear had a significant effect.

Phillips et al. (1970) used the Euler-Bernoulli theory and the Rayleigh-Ritz method to formulate the forced vibration of tree limbs having variable cross-sections. They also investigated various methods to model secondary branches and programmed a computer algorithm to determine the vibrational characteristic of limbs with secondary branches. Hussain et al. (1975), Ruff et al. (1980), Upadhyaya and Cooke (1981), and Upadhyaya et al. (1981b) studied the fruit-stem system using Lagrange's equation. Upadhyaya et al. (1981a, 1981b) used the Galerkin approach to solve the partial differential equations formulated based on the Bernoulli-Euler beam theory. The transient response of the limb under the base impact was solved using Newmark's direct integration method. Adrian and Fridley (1965) modeled the tree limbs as a single degree of freedom cantilever beam with viscous damping. Ebner and Billington (1968) investigated the response of an internally damped non-uniform beam under force vibrations. Hoag et al. (1970) studied the effects of proportional damping (internal damping proportional to stiffness or mass distribution), non-proportional damping

(external damping proportional to the leaf distribution), and non-linear external damping (or viscous damping), which is proportional to the  $n$ th power of the velocity of the system, on the dynamic response of tree limbs.

Computer simulation provides an efficient tool for determining the response of the whole tree to practically any vibratory force by dividing the tree into a large number of small element sections, with the mass and stiffness properties of each section known from measurements (Phillips et al. 1970; Yung and Fridley, 1975; Savary et al., 2010, 2011). However, it is unlikely that a harvester designed based on the response of a few trees will perform satisfactorily for all other trees. Thus, instead of analyzing a whole tree, this research used limb prototypes, which are non-physical representations of actual tree limbs. These limb prototypes were derived from random individual trees using statistical methods. This process involves prediction of the parameters of the primary limbs (main scaffold branches of a tree) based on statistical information accumulated from a large number of trees. In this study, a tree limb originating from the truck of a tree and having a base diameter greater than 6.35 cm (2.5 in.) is classified as a primary limb of the tree.

The proposed methodology for modeling a tree limb was used in the optimization of a continuous citrus canopy harvester. Continuous canopy shakers are currently the most widely used type of mechanical harvesting system for citrus in Florida and are primarily used to harvest oranges. Continuous canopy shakers have gained popularity and acceptance over other shakers because they do not stop at each tree during harvest and provide a high harvesting yield of approximately 95% to 96% (Whitney, 1999). However, their operation causes excessive tree damage, which results in low yield in subsequent years (Spann and Danyluk, 2010). In order to address growers' concerns about tree damage and the efficiency of the harvesting system, an economical way of defining the interactions and proposing an optimal set of machine parameters is essential.

Thus, a numerical optimization based design approach is proposed to predict an optimal set of machine parameters that minimize tree damage and maximize fruit removal. The methodology involves determining properties of the wood, forming statistical models of tree limbs, performing dynamic analysis, and building mechanistic models to mathematically define the objective functions of optimization, as shown in figure 1. This article presents part of the research work describing the first two steps involved in the

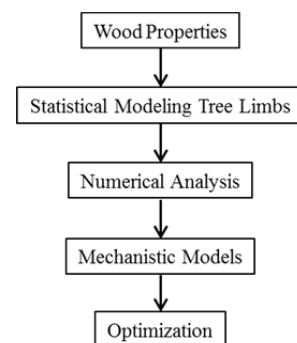


Figure 1. Schematic of processes involved in optimization of shaker.

numerical-based design optimization of a canopy shaker, whereas other steps are presented by Gupta et al. (2015).

## MATERIALS AND METHODS

The following sections describe the methodology used to determine the material properties, collect data on tree limbs from citrus trees, and model the prototypes of the primary limb.

### CONTINUOUS CANOPY SHAKER: CURRENT HARVESTING SYSTEM FOR CITRUS

The current mechanical harvesting system used to harvest citrus fruits in Florida is a continuous canopy shaker, which is an enhanced version of the design proposed by Peterson (1998). There are two versions of this system: (1) the continuous canopy shake and catch harvester (fig. 2), which has a catch frame for collecting harvested fruits, and (2) the tractor-drawn canopy shaker (fig. 3), which is only equipped to detach the fruits; the detached fruits are then picked up from the ground manually or by pickup machines. The principle mechanism used to detach the fruits is the same in both harvesters and is accomplished by periodically impacting the tree limbs with sinusoidally vibrating tines. The tines are 198.12 cm (78 in.) long and arranged radially on 12 wheels mounted on a cylindrical frame, as shown in figures 2 and 3. The sinusoidal motion of the tines is provided by a slider crank mechanism, which is powered by a hydraulic motor.



Figure 2. Continuous canopy shake and catch harvester (photo courtesy of Ehsani and Sajith).



Figure 3. Tractor-drawn canopy shaker harvester (source: <http://citrusmh.ifas.ufl.edu/images/history/current/025.jpg>).

## MEASURING MATERIAL PROPERTIES OF CITRUS WOOD

The material properties of the wood were determined from fresh samples taken randomly from the different primary limbs of Valencia (*Citrus sinensis*) orange varieties grown at the University of Florida Citrus Research and Education Center (CREC). The samples were machined to the sizes recommended by ASTM Standard D143-09 (ASTM, 2009). The dimensions were measured at the two ends and at the center of the specimen using electronic digital calipers with a resolution of 0.0127 mm (0.0005 in.). The mean values were used in the calculations of the wood properties. The average values of the mechanical and physical properties of citrus wood were used in the numerical model.

### Mechanical Properties

Three-point bending tests were performed on six wood samples machined to a width of 3.81 cm, a height of 2.54 cm, and a length of 45.72 cm (1.5 in.  $\times$  1 in.  $\times$  18 in.) using a universal testing machine (model 313R electromechanical PC-based tabletop test system, TestResources, Inc., Shakopee, Minn.). The samples were simply supported between the knife edges of the three-point bending support, as shown in figure 4. The crosshead of the instrument was adjusted to come in proper contact to the top surface at the mid-plane of the sample. The load was applied continuously throughout the test at a rate of motion of the movable crosshead of 2.54 mm  $\text{min}^{-1}$  (0.1 in.  $\text{min}^{-1}$ ). The load cell of the instrument was set to continuously record the reaction force until the specimen fractured or failed to support a bending load of 2.22 kN (500 lbf). The fracture due to static bending failure was identified as the appearance of brush or fiber delamination of the wood specimen. Load-deflection data were acquired from each specimen using TestResources R-series software. The wood was assumed to be isotropic and homogenous, and the mechanical properties were determined from the load-deflection curve.

The modulus of elasticity ( $E$ ) was calculated from the load-deflection ( $P-\delta$ ) curves of specimens using equation 1. The bending moment ( $M$ ) and modulus of rupture

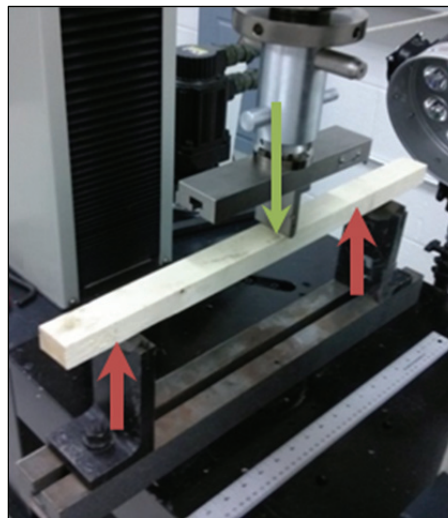


Figure 4. Three-point bending test of a citrus wood specimen (photo courtesy of Gupta).

( $R$ ) were calculated using equations 2 and 3, respectively. The modulus of rupture is an accepted criterion of strength for wood, is equivalent to the fracture stress, and reflects the maximum load-bearing capacity during bending. The stress at the proportional limit ( $\sigma_{PL}$ ) is the stress proportional to the load at which the load-deflection curve is a straight line and was calculated using equation 4. The work to maximum load ( $W_{ML}$ ) in bending is the ability of wood to absorb shock with some permanent deformation. It determines the combined strength and toughness of wood under bending stress and was calculated using equation 5:

$$E = \frac{ML^2}{12I\delta} \quad (1)$$

$$M = \frac{PL}{4} \quad (2)$$

$$R = \frac{3P_{max}L}{2bd^2} \quad (3)$$

$$\sigma_{PL} = \frac{3P_{PL}L}{2bd^2} \quad (4)$$

$$W_{ML} = \frac{A}{bdL} \quad (5)$$

where  $M$  is the bending moment,  $I$  is the moment of inertia,  $L$  is the length of the specimen,  $\delta$  is the deflection at the mid-span of the specimen,  $A$  is the area under the  $P$ - $\delta$  curve up to the maximum load,  $b$  is the width of the specimen,  $h$  is the height of the specimen, and  $P_{PL}$  is the load at the proportionality limit.

### Density

Three samples of citrus wood were cut from the specimens used in the bending test and tested to determine the density of green citrus wood. The change in the pressure values of the chamber with or without the specimen obtained using a pycnometer (Ultra-Pycnometer 1000, Quantachrome Corp., Boynton Beach, Fla.) were used to calculate the volume, and subsequently the density, of the specimens using equation 6:

$$V_{sample} = \frac{(P_A - P_B)V_{cell} - P_B V_{added}}{P_A - P_B} \quad (6)$$

where  $V_{sample}$  is the unknown volume of the specimen,  $V_{cell}$  is the known volume of the cell,  $V_{added}$  is the known volume of an additional chamber,  $P_A$  is the equilibrium pressure in the helium tank or sample cell, and  $P_B$  is the cell pressure when the cell communicates with an additional chamber. The instrument was calibrated prior to the experiments with a sphere of a known volume. Each sample was tested five times, and the value of density, calculated using equation 7, was averaged:

$$\rho = \frac{Mass_{sample}}{V_{sample}} = \frac{(P_A - P_B)Mass_{sample}}{(P_A - P_B)V_{cell} - P_B V_{added}} \quad (7)$$

### Moisture Content

The moisture content of the green citrus wood samples is not required in the numerical model; however, their mechanical behavior varies with respect to water content. Based on Wilson (1932), the mechanical properties of wood, such as modulus of rupture, fiber stress at the elastic limit in bending, flexural modulus, and fiber stress at 3% deformation, vary with moisture content below the fiber saturation point and become invariant above this point. Wangaard (1950) defined the "fiber saturation point" of wood as the point at which all the free water in the cell cavity has been removed but the cells are still fully saturated. For most woods, the fiber saturation point lies between 25% and 30%. Thus, it is essential to know the moisture content of the samples used in the bending test. The moisture content should be greater than the fiber saturation point in order to accurately simulate the physical phenomena using a numerical model. Nine samples were cut from the bending test specimens and were dried at a temperature of 105°C until no significant decrease in mass was noticed. The mass of wood corresponding to this point is called the oven-dry mass. The moisture content of the specimens was determined from the loss in mass and was expressed in percent of the oven-dry mass as:

$$\text{Moisture content (\%)} = \frac{m_{wet} - m_{dry}}{m_{dry}} \times 100 \quad (8)$$

### Damping Coefficient

The dynamic responses of tree limbs, unlike other mechanical structures, are greatly affected by the amount and type of damping present in the system (Hoag et al., 1970, 1971). The amount of damping determines the ratio of vibrational energy dissipated and the amount of energy transferred from the harvesting machine to the fruit-bearing branches of the tree. Physically, the damping can be internal, i.e., inherent in the wood and bark, or external due to air resistance. The viscous damping due to air drag on the secondary branches, twigs, leaves, and fruits contributes significantly to the damping of tree crops and is mathematically convenient to model because only formulation of a linear second-order differential equation is required. Therefore, equivalent viscous damping, which models the overall damped behavior of a structural system as viscous, was employed (Thomson, 1993). The damping is expressed in terms of the damping ratio ( $\zeta$ ), which is the ratio of the damping of the system normalized to the critical damping ( $c_0$ ), as given in equation 9. A system is said to be underdamped if  $\zeta < 1$ , critically damped if  $\zeta = 1$ , and overdamped if  $\zeta > 1$ . For a single degree of freedom (SDOF), an underdamped system subjected to an impulse of time ( $t$ ) exhibits a response  $x(t)$ , as shown in figure 5, and decays exponentially as given by equation 10, where  $w_d$  is the natural frequency of the system, and  $x(0)$  is the displacement at  $t = 0$ . The logarithmic decrement method is a widely used method of measuring the damping ratio ( $\zeta$ ) of a system as the rate of decay of response for consecutive cycles of the vibration, which is referred to as the log decrement ( $\delta$ ). Equations 11 and 12 are used to determine the log decrement and the damping ratio of a system, respectively:

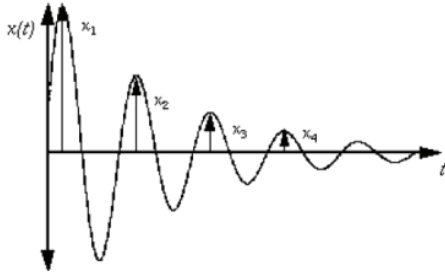


Figure 5. Underdamped response of a system having a SDOF.

$$\zeta = \frac{c}{c_0} \quad (9)$$

$$x(t) = x_0 e^{-\zeta \omega_n t} \sin \omega_d t \quad (10)$$

$$\delta = \frac{1}{n} \left( \frac{X_i}{X_{i+n}} \right) = \frac{2\pi\zeta}{\sqrt{1-\zeta^2}} \quad (11)$$

$$\zeta = \frac{\delta}{\sqrt{4\pi^2 + \delta^2}} \quad (12)$$

An experiment was set up in the CREC research orchard to measure the damping of the tree limbs of a citrus crop. The response of the tree limbs under dynamic testing was measured using an accelerometer (Horvarth and Sitkei, 2005; Chopra, 1995). Two primary limbs each from the top, middle, and bottom sections of the citrus tree canopies were randomly selected, and accelerometers (X250-2 data logger, Gulf Coast Data Concepts LLC, Waveland, Miss.) were installed as shown in figure 6. Three accelerometers were mounted on each primary limb at the tip, middle of the limb, and near the origin of the primary limb from the trunk. The tips of the primary limbs were laterally displaced to approximately 76.2 cm (30 in.) using an in-house quick-release mechanism that allowed the limbs to vibrate naturally. The responses of the primary limbs were acquired using an accelerometer data logger, and the experiments were repeated three times for each primary limb. The damping ratio was estimated using the logarithmic decrement method given by equations 11 and 12.



Figure 6. Accelerometer mounted on primary limb of a citrus tree.

## MODELING OF LIMB PROTOTYPES

The information gathered during the field experiment was used to predict the configuration of statistical prototypes of the tree limbs. Response surface models (or surrogate models) were designed to predict the sectional properties of the tree limb prototypes. The citrus tree limbs measured in the field experiment were first classified into multiple sets or zones based on the vibration transmissibility. The vibration transmissibility of a tree limb is defined as the ability of the limb to transmit energy from the point of excitation to the fruit-bearing regions and is a function of mass, stiffness, and damping, which in turn depends on the configuration of the tree limb (spatial coordinates and location of fruit-bearing regions) and the material properties of the wood (O'Brien et al., 1983). Tree limbs, having different vibration transmissibilities, require different shaking inputs to detach the fruits. Therefore, a vibratory harvester equipped to provide multiple values of shaking force can effectively minimize tree damage and maximize fruit removal. However, only three sets of machine configurations, providing three different shaking forces, were proposed in this research to minimize computational time and manufacturing costs.

## INTERPOLATING TECHNIQUE: CONTINUOUS PIECEWISE CUBIC HERMITE INTERPOLATION

Piecewise cubic Hermite interpolating polynomial (PCHIP) is an interpolation technique based on piecewise polynomials. These are shape-preserving piecewise cubic polynomials whose first-order derivatives are continuous and are used to generate smooth curves passing through a series of input data points. The polynomial function  $P(x)$  on the interval  $x_k \leq x \leq x_{k+1}$  is expressed in terms of local variables  $s = x - x_k$  and  $h = h_k$  as:

$$P(x) = \frac{3hs^2 - 2s^3}{h^3} y_{k+1} + \frac{h^3 - 3hs^2 + 2s^3}{h^3} y_k + \frac{s^2(s-h)}{h^2} d_{k+1} + \frac{s(s-h)^2}{h^2} d_k \quad (13)$$

$$\begin{aligned} P(x_k) &= y_k, & P(x_{k+1}) &= y_k \\ P'(x_k) &= y_k, & P'(x_{k+1}) &= y_k \end{aligned} \quad (14)$$

The inbuilt MATLAB function “pchip” was used to construct a Hermite interpolation passing through data points using the polynomial given in equation 13 and satisfying the conditions given by equation 14.

## RESPONSE SURFACE METHODOLOGY: POLYNOMIAL RESPONSE SURFACE

The polynomial response surface (PRS) approximation is a response surface method that uses polynomial functions to predict the best fit for the measured data to predict the true response of the system (Viana et al., 2009). The parameters of an approximate polynomial function are determined using the least squares method. A second-degree polynomial model is expressed in equations 15 and 16:

$$\hat{y} = \beta_0 + \sum_{i=1}^k \beta_i x_i + \sum_{i < j} \sum_{i=1}^k \beta_{ij} x_i x_j + \sum_{i=1}^k \beta_{ij} x_i^2 \quad (15)$$

$$e = y - \hat{y} \quad (16)$$

where  $\{x\} = [x_1, x_2, x_3, x_4, \dots, x_k]^T$ , and  $\{\beta\}$  is a vector of constant coefficients obtained by the minimizing the residual error  $\{e\}$  between the prediction  $\{\hat{y}\}$  and data  $\{y\}$

### RESIDUAL ANALYSIS: CROSS-VALIDATION ERROR

Cross-validation error is the error at a data point when the response surface (also called surrogate model) is fitted to a subset of the data points not including that data point (Allen, 1971; Khuri and Cornell, 1996). A vector of error ( $e_p$ ) is obtained by repeatedly fitting the response surface using  $n-1$  points and evaluating the error at the dropped data for all  $n$  data. This vector of error is called the cross-validation error or the prediction residual sum of squares (PRESS) error. This measure is most often used in calculating the predictive capability of a response surface as  $PRESS_{RMS}$ , which is the root mean square of the PRESS error. The prediction error at each dropped data point is given by equation 17 where  $E_{ii}$  is the diagonal matrix of the term  $E$  as defined in equation 18. The  $PRESS_{RMS}$  is then computed using equation 19:

$$e_{pi} = \frac{e_{ri}}{1 - E_{ii}} \quad (17)$$

$$E = X(X^T X)^{-1} X^T \quad (18)$$

$$PRESS_{RMS} = \sqrt{\frac{1}{n} e_p^T e_p} \quad (19)$$

### EXPERIMENTAL SETUP: ACQUIRING DATA FOR THE STATISTICAL MODEL

The tree limb configuration or tree limb parameters must be defined in order to analytically model a tree limb. The true dynamic response of a tree limb with an infinite amount of degrees of freedom is approximated by modeling

the limb as a finite set of elements in the numerical method. Information about the distribution of the secondary branches and fruits must be included in the numerical model, as they considerably modify the dynamic response of tree limbs by changing the overall mass and dissipative properties of the primary limbs.

A field experiment was set up to provide the following information to model and analyze the tree limbs using FE methods:

- Spatial coordinates of the primary limbs.
- Sectional property along the length of the primary limbs and secondary branches.
- Distribution of secondary branches on the primary limbs.
- Distribution of the fruits on the primary limbs.

The tree data were collected from 54 primary limbs of ten randomly chosen medium-sized trees of the Valencia orange variety (*Citrus sinensis*) at the CREC research orchard from 28 February 2013 to 8 March 2013. A referenced system based on Cartesian coordinates with the origin at the trunk base was employed to measure the tree limb characteristics, as shown in figure 7a. The following information was used to model the tree limbs: the length of the limb segments between two branching nodes, the angle from the z-axis (called the vertical angle), and the angle from the Y-Z plane (called the horizontal angle).

### Procedure

The following procedures were used during measurement of the tree limb parameters:

- The primary limbs were discretized into nodes (junctions where a branch splits into two or more branches), which were either the point of origin of a secondary branch or another primary limb.
- The length, vertical angle, and horizontal angle of each segment of the primary limbs were measured.
- The sectional perimeters of each limb segment were measured near the branching nodes and at the center of the segment.
- The overall length, vertical angle, and horizontal angle of all secondary branches were measured.

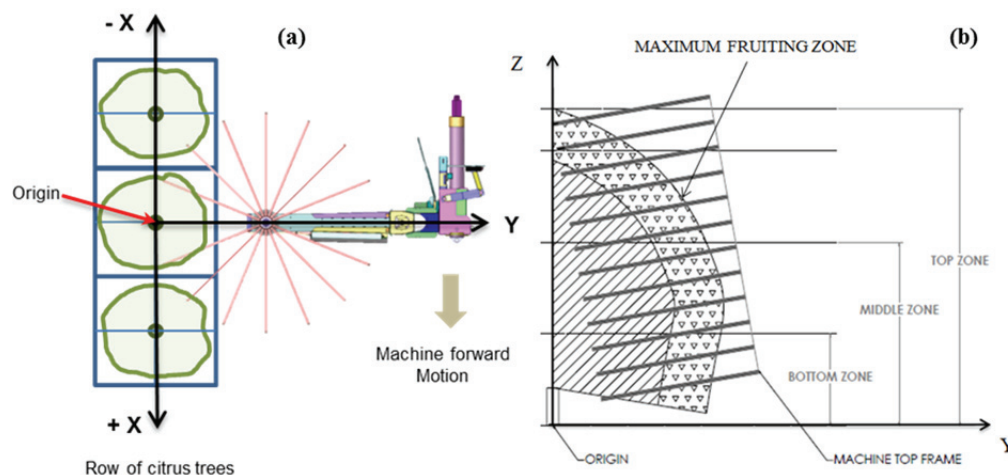


Figure 7. (a) Interaction of machine with a row of citrus trees and (b) set of tines in Y-Z plane interacting with primary limbs of citrus canopy.

- The sectional perimeters at the origin, center point, and tip of the secondary branches were measured.
- The fruits on the secondary branches and on the last segment of the primary limbs were counted.

### Assumptions

The following assumptions were made to predict the configuration of the statistical limb prototypes:

- The sections of the primary limbs and secondary branches were assumed to be circular.
- A branch originating from a primary limb and having base diameter greater than 2.54 cm (1 in.) and less than 6.35 cm (2.5 in.) was considered a secondary branch.
- The twigs, stems, and leaves were not considered explicitly in the numerical model, but their effect on the dynamic response of the primary limbs was modeled using viscous damping.

### CLASSIFICATION OF PRIMARY TREE LIMBS

The primary limbs measured in the field were modeled using a program designed in MATLAB 2011 (Math Works, Natick, Mass.) and classified into three sets based on the spatial configuration of their fruit-bearing regions (the last segment of a primary limb that generally bears the most fruits). Equation 20 was used to classify the primary limbs into three zones, referred to as the top, middle, and bottom zones:

Top zone:  $H_{FBR} > 2.29$  m (90 in.)

Middle zone:  $1.14$  m (45 in.)  $\leq H_{FBR} \leq 2.29$  m (90 in.) (20)

Bottom zone:  $H_{FBR} \leq 1.14$  m (45 in.)

where  $H_{FBR}$  is the height of the fruit-bearing region or tip of the tree limb above ground level.

### PREDICTION OF SPATIAL COORDINATES OF LIMB PROTOTYPES

A canopy shaker interacts predominantly with the primary limbs in the plane of the tines ( $Y$ - $Z$ ), as shown in figure 7b; therefore, it is numerically economical to model the limbs as a two-dimensional FE, as shown in figure 8a and 8b. Figure 8b shows how a sinusoidal vibrating tine with forward motion in the  $x$ -direction interacts with a primary limb. The measured three-dimensional limb data were projected onto a rotated  $Y$ - $Z$  plane, and the projected data were then used to construct the two-dimensional tree limbs, as shown in figure 8a. It is also feasible to model the tree limbs as a three-dimensional FE by adding a few more parameters, but the improvement in the results will barely justify the computational expenses for modeling and analyzing the limbs. The interpolating polynomial, PCHIP, was used to create the smooth and continuous differential curve passing through measured data points to model the primary limbs. The interpolated primary limbs were then used to predict the spatial coordinates of the tree limb prototype, which is a non-physical representation of an actual tree limb. The following procedure was adopted for modeling a statistical limb prototype:

- An axis ( $y$  or  $z$ ) having the maximum coordinate val-

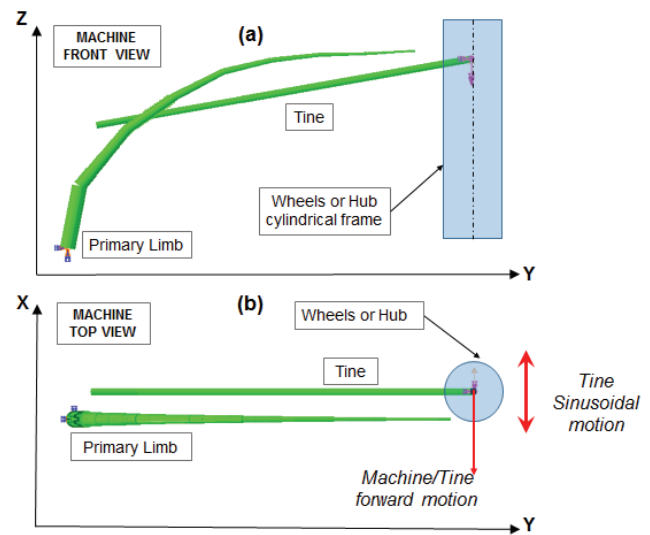


Figure 8. Interaction between a tine and a primary limb: (a) how the tine interacts with a primary limb and (b) the direction of forward and sinusoidal motion of the tine.

ue for any primary limbs in a zone was chosen as the primary axis for that zone, and the other axis is referred as the secondary axis.

- Equally spaced points were generated between the minimum and maximum coordinate values of the primary axis for each zone. Figure 9 shows the equally spaced points  $x_1 \dots x_i \dots x_n$  on the primary axis. In this study,  $n = 30$  coordinate values were chosen along the  $z$ -axis for the top zone and along the  $y$ -axis for the middle and bottom zones.
- The parameters of the PCHIP interpolating function were predicted for each primary limb.
- The coordinate value along the secondary axis corresponding to a predefined coordinate value along the primary axis was predicted using the PCHIP parameters calculated for each primary limb.
- Five limb prototypes per zone were designed and assumed to behave collectively and respond similarly to the different type of limbs spatially distributed in that zone. It would be beneficial to design an infinite number of limbs in each zone and then optimize the tine based on the overall dynamic response of the primary limbs of that zone; however, that would be extremely challenging. Thus, a few limb prototypes were statistically designed from the measured limb data to approximate the responses of the limbs in the zone.
- Assuming a normal distribution of the secondary axis coordinate values calculated from PCHIP at the  $x_1 \dots x_i \dots x_n$  locations on the primary axis, the 5th, 25th, 50th, 75th, and 95th percentile values of the secondary coordinates were predicted in each zone.
- The five limb prototypes were constructed for each zone by joining the 5th, 25th, 50th, 75th, and 95th percentile data from the normal distribution. Figure 9 shows how 25th, 50th, and 75th percentile limb prototypes were constructed.

Thus, considering five limb prototypes per zone in the optimization of the canopy shaker appropriately balances

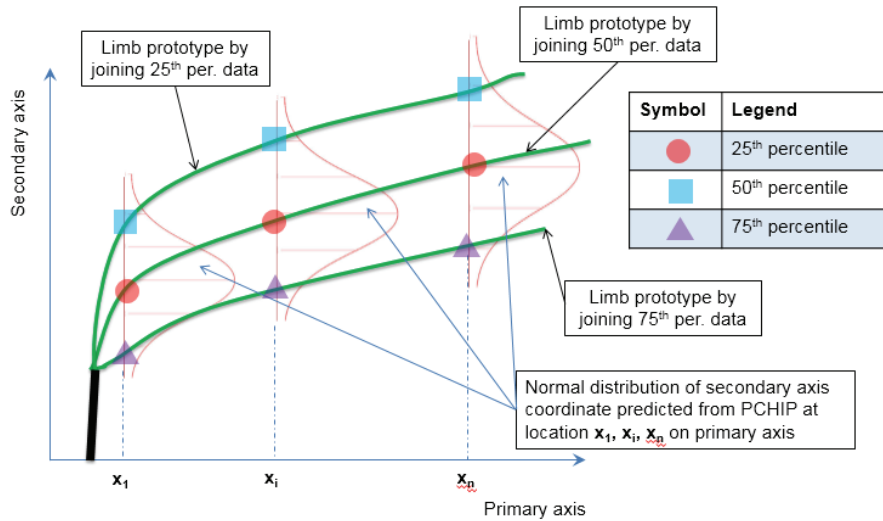


Figure 9. Method used to construct statistical limb prototypes from measured limb data.

the cost of computation in FE analysis and the statistical variation in the dynamic responses of the tree limbs.

### PREDICTION OF SECTIONAL PROPERTIES OF LIMB PROTOTYPES

The dynamic response of the limb is a function of the intrinsic properties of the limb, such as stiffness, mass, and moisture content, and the input energy characteristic. The stiffness of the limb, in turn, is a function of the sectional diameter of the limb. Therefore, the sectional diameter of the limb prototypes needed to be calculated to predict their dynamic response using FEM for the optimization of the canopy shaker. The perimeter measured along the primary limbs was used to calculate the sectional diameter of the limb prototypes, assuming a circular cross-section. It was observed that the diameter of a tree limb at any section decreases as the distance of the section from the limb origin increases. In addition, the sectional diameter along the length of a tree limb varies depending on the spatial orientation of the limb in the tree structure. Thus, it was concluded that the diameter of a tree limb at any cross-section depends on the actual distance of the cross-section from the limb origin and the angle made by the position vector joining the location of the cross-section and the limb origin, as shown in figure 10. Mathematically, this relationship is

expressed in equation 21:

$$D = f(L_n, \beta_n) \quad (21)$$

where  $L_n$  is the actual length of the  $n$ th branching node from the limb origin, and  $\beta$  is the vertical angle of the position vector joining the  $n$ th node with the limb origin. The actual distance of a branching node and the vertical angle of the position vector joining that branching node with the limb origin were measured for all primary limbs and used to predict the sectional diameters of the limb prototypes.

A polynomial response surface was employed to fit the measured data and predict the diameter of a limb prototype. The SURROGATES toolbox (Viana, 2010) was used to create response surfaces with full and stepwise regression. The response surface with full regression involves all coefficient terms of a polynomial response surface, whereas stepwise regression only involves coefficient terms having  $|t\text{-statistics}| \geq 1$ . The response surfaces were selected based on the indicator of predictive performance and the indicator of quality of fit, i.e., cross-validation error ( $PRESS_{RMS}$ ) and adjusted coefficient of correlation ( $R^2$ ), respectively.

### DISTRIBUTION OF SECONDARY BRANCHES

The secondary branches modify the dynamic response by changing the overall mass and dissipative properties of the primary limb. The overall length, circumference, and coordinates of the origin of the secondary branch were measured. Based on field observation and data analysis, it was found that approximately four or five secondary branches radiate from the primary limb at the intervals of approximately 50.8 to 63.5 cm (20 to 25 in.). This information was used to add a secondary branch effect in the numerical model.

### DISTRIBUTION OF FRUITS ON PRIMARY LIMBS

Including the effect of fruits is pivotal in determining the dynamic response of a fruit-bearing limb under vibratory excitation. The fruits act as an inertial damper and attenuate the dynamic responses of the limbs. The distribution of fruits on a primary limb can be classified into two groups:

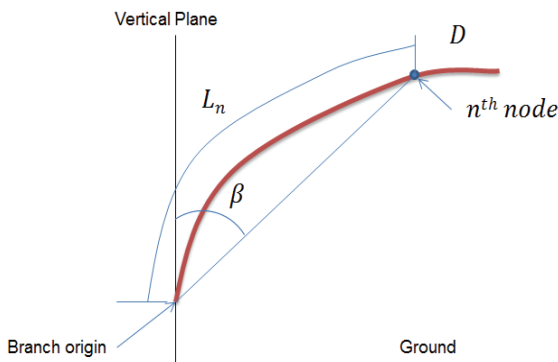


Figure 10. Diameter of a primary limb at any branching node as a function of the length and the angle of that node from the limb origin.

- Fruits attached to the secondary branches of the primary limb.
- Fruits attached to the last segment, called the fruit-bearing region, of the primary limb.

### Fruits on Secondary Branches

The number of fruits on the secondary branches was counted. The average mass of orange fruit (0.186 kg) was used to compute the total mass of fruits on the secondary branches of the primary limb.

### Fruits in Fruit-Bearing Region

The fruit-bearing region of a primary limb is the region near the tip of the limb where the limb branches into a large number of small twigs and bears a large number of fruits. Information regarding the configuration and number of fruits in the fruit-bearing region is significant, as numerical models are evaluated in these regions of the primary limbs to optimize the parameters of a canopy shaker.

## RESULTS AND DISCUSSION

The current problem of canopy shaker optimization has two competing objectives: minimum tree damage and maximum fruit removal (Gupta et al., 2015). The machine parameters, such as tine configuration and operating parameters, should be designed to minimize tree damage without compromising fruit removal. For example, stiffening the tines would result in higher fruit removal, as it would transfer higher vibrational energy to the limb; however, this would also cause higher stresses in the limb and thus more damage. Thus, the problem results in a non-dominated, Pareto-optimal, or non-inferior solution because none of the objective functions can be improved in value without degrading other objective values (Pareto, 1971). In addition, it is not only uneconomical but also overly conservative to optimize the canopy shaker parameters for the worst-case condition, which protects every tree limb. Therefore, the average values of the tree parameters have been taken to represent “typical trees” in the optimization of the canopy shaker to save not every limb but the maximum possible tree limbs. This is achieved by calculating the mean assuming a normal distribution of the tree parameters, such as mechanical and physical properties, spatial distribution of limbs, and distribution of the secondary branches and fruit mass.

### MECHANICAL PROPERTIES

A summary of the mechanical properties calculated from the three-point bending test is presented in table 1. The means and coefficients of variation (CV) of the mechanical properties were calculated from the load-deflection curves shown in figure 11 using equations 1 to 5. The elastic modulus and modulus of rupture were used in this research for the formulation of the numerical model. The other two properties provide knowledge of the elastic behavior and shock absorbing capacity of the citrus wood. Figure 11 shows the best fit curve and the load-deflection curves from the bending tests of the citrus wood samples.

**Table 1. Summary of mechanical properties of green citrus wood.**

Mechanical Property	Mean	CV
Flexural modulus (GPa)	8.5	11%
Modulus of rupture (MPa)	67.3	4%
Stress at proportional limit (MPa)	45.3	13%
Work to maximum load in bending ( $\text{kJ m}^{-3}$ )	193.2	28%

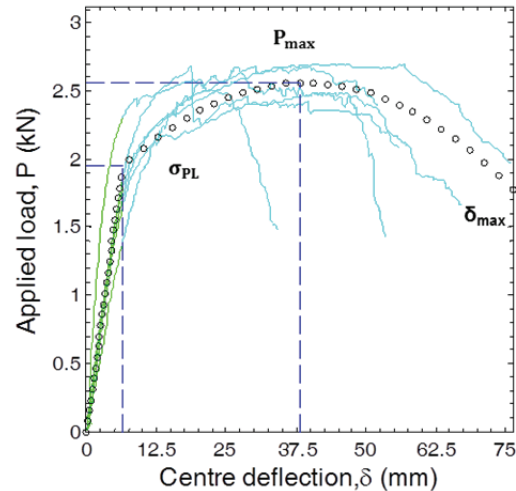


**Figure 11. Best fit and load-deflection curves of green citrus wood.**

### PHYSICAL PROPERTIES

A summary of the measured physical properties is presented in table 2. The mean and coefficient of variation (CV) are reported for each property. It was found that the moisture content of the samples used in the bending test was greater than the fiber saturation point, indicating that the measured mechanical properties of the citrus wood are invariant with moisture content and thus can be used in the numerical formulation. Figure 12 shows the underdamped response of a citrus limb when displaced and allowed to vibrate naturally. The average value of the viscous damping ratio of citrus limbs was found to be approximately 11. The high value of the damping ratio suggests that the damping in tree limbs is highly dependent on the air drag on fruits, leaves, and twigs (viscous damping) rather than the material properties of the wood (structural damping). The friction coefficient between wood and steel was not measured but

**Table 2. Summary of physical properties.**

Physical Property	Mean	CV
Density ( $\text{kg m}^{-3}$ )	1450.8	2.8%
Moisture content (%)	42.4	14.15%
Damping ratio (%)	10.78	24.70%
Friction	0.36	20.97%

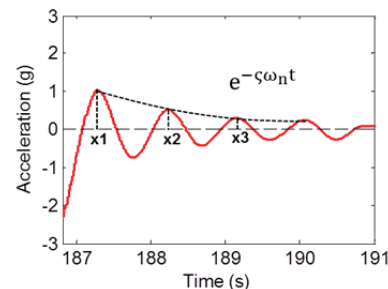


**Figure 12. Underdamped response of a citrus tree limb.**

taken from the research of McKenzie and Karpovich (1968).

### MODELING LIMB PROTOTYPES

The primary limbs were classified into three zones based on their spatial distribution in the tree canopy. The models were formulated to predict the spatial configuration and properties of the limb prototypes. The statistical information from the field measurements was analyzed and used to predict the distribution of secondary branches and fruits along the primary limbs.

### CLASSIFICATION OF PRIMARY TREE LIMBS

The primary limbs, classified into three sets, have similar dynamic responses owing to their properties, distribution of secondary branches, and configuration of the fruit-bearing region. Figure 13 shows a three-dimensional representation of the citrus primary limbs analyzed to predict the statistical limb prototypes.

### PREDICTION OF SPATIAL COORDINATES OF LIMB PROTOTYPES

Sets of representative or prototype tree limbs were defined for each zone. Figures 14a, 14b, and 14c show the spatial distribution of the limb prototypes capturing the 5th, 25th, 50th, 75th, and 95th percentiles of the primary limbs in the top, middle, and bottom zones, respectively. The dashed lines show PHCIP-interpolated limbs passing through the measured data points, which are represented by circles. It can be seen that the limbs in the top zone predominantly radiate at an angle of  $0^\circ$  to  $20^\circ$ , grow straight up to a height of 3.05 to 3.3 m (120 to 130 in.), and then curve down slightly at the tip, as shown in figure 14a. However, for the middle zone, the limbs are thick, long, and hang down gradually after growing approximately 1.22

to 1.52 m (48 to 60 in.) due to the weight of the fruits, as shown in figure 14b. The limbs in the bottom zone originate and grow near the ground and are comparatively thinner, shorter, and curve down steeply near the tip of the limb, as shown in figure 14c.

Figure 15a compares the spatial distribution of the 50th percentile tree limbs and 90% bounds of the tree limbs in the three zones. The spatial distribution of the statistical tree limb prototypes forms a half-section of a hypothetical tree structure, as shown in figure 15a. The components of shakers will be optimized based on their interaction with the limbs of this hypothetical tree structure rather than any actual tree, as shown in figure 15b. Thus, the tines that interact with limbs in the top zone have a different configuration, based on the amount of shaking force required by those limbs for minimum damage and maximum fruit removal, as compared to the tines that interact with the middle and bottom zones.

### PREDICTION OF SECTIONAL PROPERTIES OF LIMB PROTOTYPES

Tables 3 and 4 illustrate the error norms of various surrogate models formulated to predict the sectional diameters of limb prototypes in all three zones. The surrogate model that had the lowest cross-validation error and the highest adjusted  $R^2$  was chosen as the best fitting model for each zone. Thus, the third-degree polynomial response surface with stepwise regression was used for limbs in the top zone, whereas the third-degree polynomial response surface with full regression was used for limbs in the middle and bottom zones. The surrogate models, thus formulated, for predicting the diameters of limb prototypes in the top, middle, and bottom zones are given in equations 22, 23, and 24, respectively:

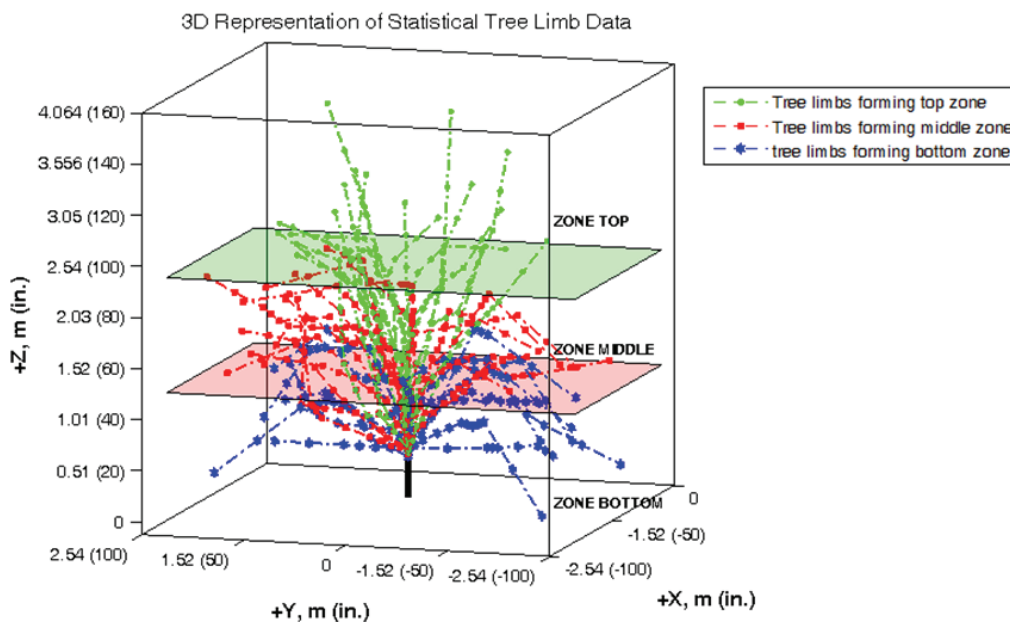


Figure 13. Three-dimensional view of citrus tree limbs and their classification into three zones.

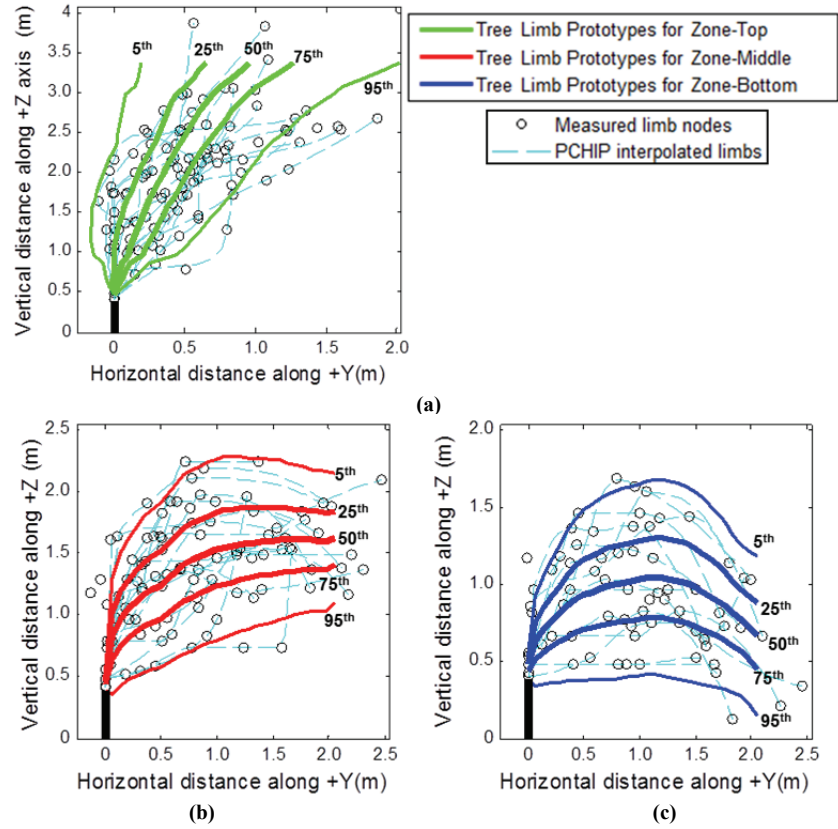


Figure 14. (a) Spatial modeling of limb prototypes for the (a) top zone, (b) middle zone, and (c) bottom zone.

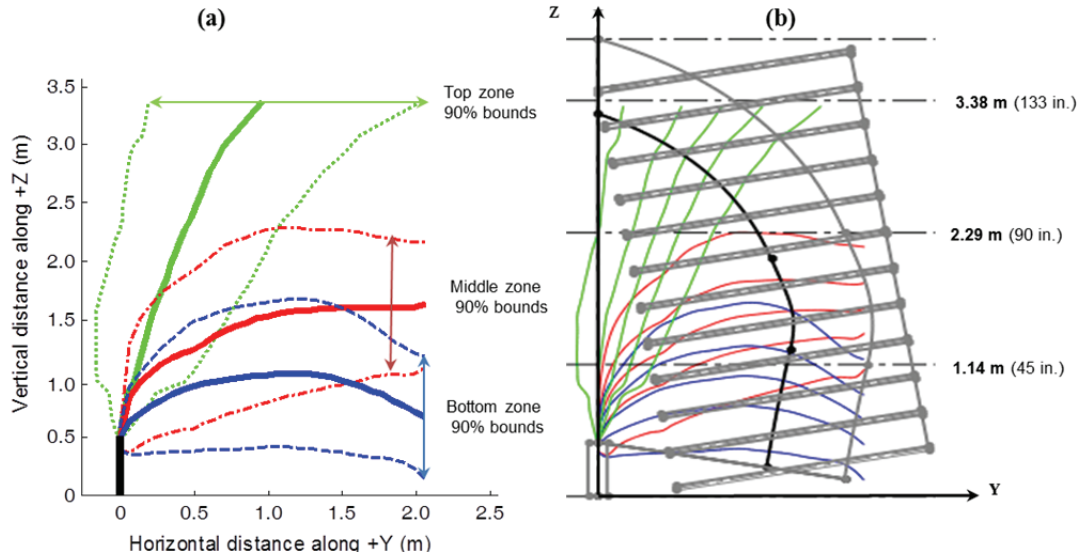


Figure 15. (a) Spatial distribution of limb prototypes of a hypothetical tree and (b) interaction of a canopy shaker with the limb prototypes.

$$\begin{aligned}
 D_{top} = & 3.9309 - 0.1044\beta + 0.0026\beta^2 + 0.0011\beta L \\
 & - 4.8262 \times 10^{-4} L^2 - 2.844 \times 10^{-5} \beta^2 L \\
 & + 2.015 \times 10^{-6} L^3
 \end{aligned} \quad (22)$$

$$\begin{aligned}
 D_{middle} = & 3.7172 - 0.0647\beta - 0.0049L + 7.6411 \times 10^{-4} \beta^2 \\
 & + 3.7797 \times 10^{-4} \beta L - 2.9258 \times 10^{-4} L^2 \\
 & + 8.8872 \times 10^{-6} \beta^3 - 1.9091 \times 10^{-5} \beta^2 L \\
 & + 6.1894 \times 10^{-6} \beta L^2 + 4.1649 \times 10^{-7} L^3
 \end{aligned} \quad (23)$$

**Table 3. Surrogate model to predict the diameter of limbs of the top zone.**

Zone	Error Norm	PRS-Linear, Full Regression	PRS-Quadratic, Stepwise Regression	PRS-Cubic, Stepwise Regression	PRS-Quartic, Full Regression
Top	PRESS <sub>RMS</sub> (%)	9.4	9.1	8.8	8.9
	Adjusted R <sup>2</sup> (%)	86.5	87.3	88.2	88.0

**Table 4. Surrogate models to predict the diameter of limbs of the middle and bottom zone.**

Zone	Error Norm	PRS-Linear, Full Regression	PRS-Quadratic, Stepwise Regression	PRS-Cubic, Full Regression	PRS-Quartic, Full Regression
Middle	PRESS <sub>RMS</sub> (%)	10.6	10.0	9.9	10.0
	Adjusted R <sup>2</sup> (%)	80.7	82.9	83.2	83.0
Bottom	PRESS <sub>RMS</sub> (%)	9.6	8.9	8.8	8.9
	Adjusted R <sup>2</sup> (%)	81.1	84	84.7	84.5

$$\begin{aligned}
 D_{bottom} = & 2.5841 - 0.0645\beta + 0.0357L + 0.0013\beta^2 \\
 & - 6.8739 \times 10^{-4}\beta L - 3.9263 \times 10^{-4}L^2 \\
 & + 5.2031 \times 10^{-6}\beta^3 - 2.0646 \times 10^{-5}\beta^2L \\
 & + 1.6265 \times 10^{-5}\beta L^2 - 1.6425 \times 10^{-6}L^3
 \end{aligned}
 \tag{24}$$

where the diameter ( $D$ ) and length ( $L$ ) are in inches, and angle  $\beta$  is in degrees.

**DISTRIBUTION OF SECONDARY BRANCHES AND FRUITS ON PRIMARY LIMBS**

Modeling secondary branches and performing dynamic simulations is expensive; thus, the numerical model was simplified by aggregating the mass of the secondary branches and fruits on the primary limbs. This was done based on the study by Phillips et al. (1970) to simplify the computation in FE analysis. In addition, a preliminary FE analysis was performed to analyze the effect of modeling the secondary branches and fruits as a lumped mass. That preliminary study concluded that mode shapes and natural frequencies differ only by fractions as compared to a model with whole fruit and secondary branches on a primary limb.

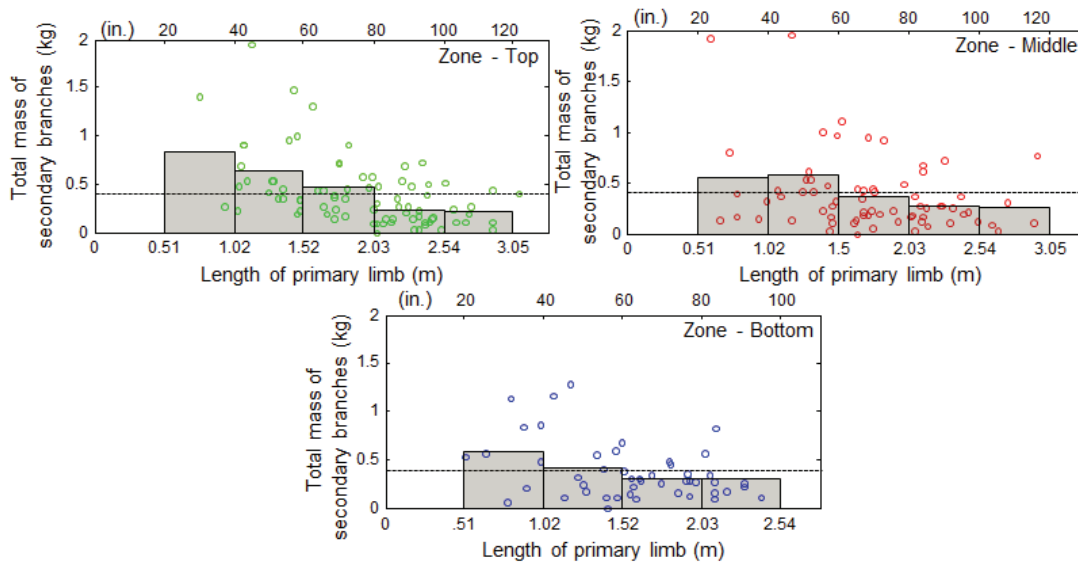
**Distribution of Secondary Branches**

Figure 16 shows the distribution of the mass of the secondary branches on the primary limbs in the top, middle,

and bottom zones. From figure 16 and the field observations, it was concluded that the secondary branches that sprout near the primary limb origin are thick and long compared to those that bud out near the tip of the primary limbs. It was observed that secondary branching of the primary limbs in the top and middle zones occurs between lengths of 50.8 to 101.6 cm (20 to 40 in.) and 254.0 to 304.8 cm (100 to 120 in.), whereas secondary branching in the bottom zone occurs between lengths of 50.8 to 101.6 cm (20 to 40 in.) and 203.2 to 254 cm (80 to 100 in.). On average, primary limbs in the top and middle zones radiate five secondary branches, whereas primary limbs in the bottom zone are shorter and sprout only four secondary branches. The average mass of the secondary branches was taken for every 50.8 cm (20 in.) segment of a primary limb and modeled at the location where the secondary branches stem out from the primary limb. The secondary branches were modeled as a lumped mass on the primary limb in the FE analysis, as presented by Phillips et al. (1970). Table 5 provides the average mass of the secondary branches in each zone. This indicates that the primary limbs in the top

**Table 5. Average mass of the secondary branches in three zones.**

Zone	Mean (kg)
Top	0.4036
Middle	0.4236
Bottom	0.3602



**Figure 16. Distribution of mass of secondary branches in three zones. Circles represent measured data.**

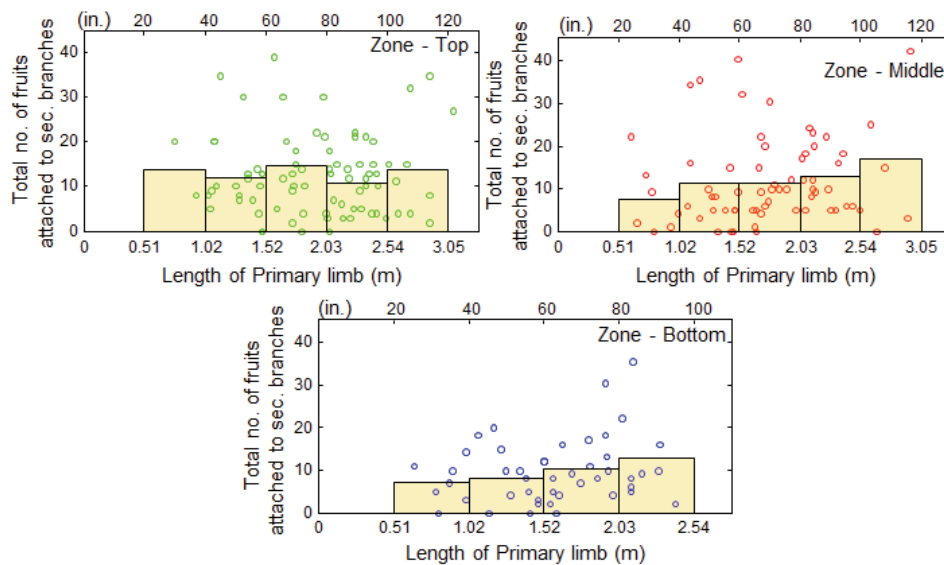


Figure 17. Distribution of fruits attached to secondary branches in three zones. Circles represent measured data.

and middle zones not only have more secondary branching but also weigh 12% and 18% more, respectively, than the secondary branches in the bottom zone.

#### Distribution of Fruits on Primary Limbs

The fruits attached to the secondary branches were modeled by aggregating their mass at the location of the secondary branches on the primary limbs. Figure 17 shows the distribution of fruits attached to the secondary branches of the primary limbs in the three zones. Table 6 provides the average number of fruits attached to the secondary branches in each zone. There is no significant variation in the distribution of fruits on the secondary branches radiating from the primary limbs for the three zones. However, the average numbers of fruits attached to secondary branches in the top and middle zones are respectively 30% and 21% more than that of the bottom zone.

Table 7 provides the information needed to configure the fruit-bearing region of a primary limb for each zone. This information is significant because the numerical model would be evaluated at these regions to optimize the shaker. It was noted that the length of the fruit-bearing region is approximately the same for almost all limbs irrespective of zone; however, the distance of the fruiting-bearing region from the limb origin is greatest for the top zone and smallest for the bottom zone. Whitney and Wheaton (1984)

showed that maximum fruiting occurs in the middle zone of citrus trees. A similar finding has been found in the current study as well with maximum fruiting occurring on the primary limbs of the middle zone, with an average fruit count that is 41% and 13% greater, respectively, than that of the top and bottom zones.

## CONCLUSION

This article presented a methodology to analytically model limb prototypes to be used in shaker optimization. The spatial coordinates of the limb prototypes were predicted based on statistical information from citrus tree limbs. Response surface methodology was used to construct models that were used to predict the sectional diameters of the limb prototypes. The secondary branches and fruits were modeled as a lumped mass on the limb prototypes to be considered while evaluating the dynamic response of the primary limbs using FE methods. The fruit-bearing regions of the primary limbs in each zone were used to quantify fruit removal in optimizing the canopy shaker (Gupta et al., 2015). The mechanical and physical properties of the citrus wood were determined from tests performed on freshly cut samples of citrus wood. The analytical models of the limb prototypes and the measured mechanical and physical properties of the wood were used to formulate finite element (FE) models of the limbs. The dynamic responses of the limbs under external excitation were predicted using a non-linear implicit FE method. The FE results were then used to optimize a continuous canopy shaker, as presented in the second part of this research (Gupta et al., 2015). We expect that this methodology will be the start of a novel way to optimize other vibratory shakers based on modeling tree limb prototypes with certain configurations and with certain known properties using numerical models. This research also demonstrates the procedure for finding the mechanical and physical properties of freshly cut wood to be used in the numerical models.

Table 6. Average number of fruits on the secondary branches.

Zone	Mean
Top	12.6
Middle	11.7
Bottom	9.7

Table 7. Configuration of fruit-bearing region in three zones.

Zone	Distance from Limb Origin, cm (in.)	Length of Fruit-bearing Region, cm (in.)	Fruit Count
Top	335.28 (132)	77.72 (30.6)	14.4
Middle	314.96 (124)	83.31 (32.8)	20.3
Bottom	284.48 (112)	82.80 (32.6)	17.9

## ACKNOWLEDGEMENTS

The authors gratefully acknowledge the Citrus Initiatives of Florida for providing research funding. We are also grateful to Dr. Peter Ifju, Dr. Arthur Teixeira, Sherrie Buchanon, Ali Mirzakhani, and Sweeb Roy for providing guidance related to material testing and data collection.

## REFERENCES

- Adrian, P. A., & Fridley, R. B. (1965). Dynamics and design criteria of inertia-type tree shakers. *Trans. ASAE*, 8(1), 12-14. <http://dx.doi.org/10.13031/2013.40414>.
- Allen, D. M. (1971). Mean square error of prediction as a criterion for selecting variables. *Technometrics*, 13(3), 469-475. <http://dx.doi.org/10.1080/00401706.1971.10488811>.
- Archer, J. S. (1965). Consistent matrix formulation of structural analysis using finite-element techniques. *AIAA J.*, 3(10), 1910-1918. <http://dx.doi.org/10.2514/3.3279>.
- ASTM. (2009). D143-09: Standard test methods for small clear specimens of timber. West Conshohocken, Pa.: ASTM.
- Chopra, A. K. (1995). *Dynamics of Structures: Theory and Applications to Earthquake Engineering*. Englewood Cliffs, N.J.: Prentice-Hall.
- Ebner, A. M., & Billington, D. P. (1968). Steady-state vibrations of damped Timoshenko beams. *J. Structural Div. ASCE* 94(3), 737-760.
- Fridley, R. B., & Adrian, P. A. (1966). Mechanical harvesting equipment for deciduous tree fruits. Bulletin 825. Berkeley, Cal.: California Agricultural Experiment Station.
- Fridley, R. B., & Lorenzen, C. (1965). Computer analysis of tree shaking. *Trans. ASAE*, 8(1), 8-11, 14. <http://dx.doi.org/10.13031/2013.40413>.
- Fridley, R. B., & Yung, C. (1975). Computer analysis of fruit detachment during tree shaking. *Trans. ASAE*, 18(3), 409-415. <http://dx.doi.org/10.13031/2013.36599>.
- Fridley, R. B., Hartmann, H. T., Mehlschau, J. J., Chen, P., & Whisler, J. (1971). Olive harvest mechanization in California. Bulletin 855. Berkeley, Cal.: California Agricultural Experiment Station.
- Futch, S. H., Whitney, J. D., Burns, J. K., & Roka, F. M. (2004). Harvesting: From manual to mechanical. Publication HS-1017. Gainesville, Fla.: University of Florida IFAS.
- Gupta, S. K., Ehsani, R., & Kim, N. H. (2015). Optimization of a citrus canopy shaker harvesting system: Mechanistic tree damage and fruit detachment model. *Trans. ASABE*, (in review).
- Halderson, J. L. (1966). Fundamental factors in mechanical cherry harvesting. *Trans. ASAE*, 9(5), 681-684. <http://dx.doi.org/10.13031/2013.40071>.
- Hoag, D. L., Hutchinson, J. R., & Fridley, R. B. (1970). Effect of proportional, non-proportional, and non-linear damping on the dynamic response of tree limbs. *Trans. ASAE*, 13(6), 879-884. <http://dx.doi.org/10.13031/2013.38742>.
- Hoag, D. L., Fridley, R. B., & Hutchinson, J. R. (1971). Experimental measurement of internal and external damping properties of tree limbs. *Trans. ASAE*, 14(1), 20-28. <http://dx.doi.org/10.13031/2013.38215>.
- Horvath, E., & Sitkei, G. (2005). Damping properties of plum trees shaken at their trunks. *Trans. ASAE*, 48(1), 19-25. <http://dx.doi.org/10.13031/2013.17936>.
- Hurty, W. C., & Rubinstein, M. F. (1964). *Dynamics of Structures*. Englewood Cliffs, N.J.: Prentice-Hall.
- Hussain, A. A. M., Rehkugler, G. E., & Gunkel, W. W. (1975). Tree limb response to a periodic discontinuous sinusoidal displacement. *Trans. ASAE*, 18(4), 614-617. <http://dx.doi.org/10.13031/2013.36644>.
- Khuri, A. I., & Cornell, J. A. (1996). *Response Surfaces: Designs and Analyses*. 2nd Ed. New York, N.Y.: Marcel Dekker.
- Markwardt, E. D., Guest, R. W., Cain, J. C., & Labelle, R. L. (1964). Mechanical cherry harvesting. *Trans. ASAE* 7(1), 70-74, 82.
- McKenzie, W. M., & Karpovich, H. (1968). The frictional behavior of wood. *Wood Sci. Tech.*, 2(2), 139-152.
- O'Brien, M., Cargill, B. F., & Fridley, R. B. (1983). *Principles and Practices for Harvesting and Handling Fruits and Nuts*. Westport, Conn.: Avi Publishing.
- Pareto, V. (1971). *Manuale di Economica Politica*. Milan, Italy: Societa Editrice Libraria. Translated into English by A. S. Schwier as *Manual of Political Economy* (A. S. Schwier and A. N. Page, Eds.). New York, N.Y.: Augustus M. Kelley.
- Pestel, E. C., & Leckie, F. A. (1963). *Matrix Methods in Elastomechanics*. New York, N.Y.: McGraw Hill.
- Peterson, D. L. (1998). Mechanical harvester for process oranges. *Applied Eng. Agric.*, 14(5), 455-458. <http://dx.doi.org/10.13031/2013.19409>.
- Peterson, D. L., Liang, T., & Myers, A. L. (1972). Feasibility study of shake harvesting macadamia nuts. In *Proc. Intl. Conf. Tropical and Subtropical Agriculture* (pp. 64-69). Special Publication SP-01-72. St. Joseph, Mich.: ASAE.
- Phillips, A. L., Hutchinson, J. R., & Fridley, R. B. (1970). Formulation of forced vibration of tree limbs with secondary branches. *Trans. ASAE*, 13(1), 138-142. <http://dx.doi.org/10.13031/2013.38553>.
- Ruff, J. H., Rohrbach, R. P., & Holmes, R. G. (1980). Analysis of the air suspension stem vibration strawberry harvesting concept. *Trans. ASAE*, 23(2), 288-297. <http://dx.doi.org/10.13031/2013.34573>.
- Rumsey, J. W. (1967a). Response of the citrus fruiting system to fruit removing actions. MS thesis. Tucson, Ariz.: University of Arizona.
- Rumsey, T. R. (1967b). Simulation of forced vibration of a tree limb by finite element methods. MS thesis. Davis, Cal.: University of California.
- Savary, S. K. J. U., Ehsani, R., Schueller, J. K., & Rajaraman, B. P. (2010). Simulation study of citrus tree canopy motion during harvesting using a canopy shaker. *Trans. ASABE*, 53(5), 1373-1381.
- Savary, S. K. J. U., Ehsani, R., Salyani, M., Hebel, M. A., & Bora, G. C. (2011). Study of force distribution in the citrus tree canopy during harvest using a continuous canopy shaker. *Computers Electronics Agric.*, 76(1), 51-58. <http://dx.doi.org/10.1016/j.compag.2011.01.005>.
- Schuler, R. T., & Bruhn, H. D. (1973). Structurally damped Timoshenko beam theory applied to vibrating tree limbs. *Trans. ASAE*, 15(5), 886-889. <http://dx.doi.org/10.13031/2013.37651>.
- Spann, T. M., & Danyluk, M. D. (2010). Mechanical harvesting increases leaf and stem debris in loads of mechanically harvested citrus fruit. *HortScience*, 45(8), 1297-1300.
- Thomson, W. T. (1993). *Theory of Vibration with Applications*. 3rd Ed. Englewood Cliffs, N.J.: Prentice-Hall.
- Upadhyaya, S. K., & Cooke, J. R. (1981). Limb impact harvesting: Part III. Model studies. *Trans. ASAE*, 24(4), 868-871, 878. <http://dx.doi.org/10.13031/2013.34354>.
- Upadhyaya, S. K., Cooke, J. R., Pellerin, R. A., & Throop, J. A. (1981a). Limb impact harvesting: Part II. Experimental approach. *Trans. ASAE*, 24(4), 864-867. <http://dx.doi.org/10.13031/2013.34353>.
- Upadhyaya, S. K., Cooke, J. R., & Rand, R. H. (1981b). Limb impact harvesting: Part I. Finite element analysis. *Trans. ASAE*, 24(4), 856-863. <http://dx.doi.org/10.13031/2013.34352>.
- Viana, F. A. C. (2010). *SURROGATES Toolbox User's Guide*. Version 3. Gainesville, Fla. Retrieved from

- <https://sites.google.com/site/srgtstoolbox/>.
- Viana, F. A. C., Haftka, R. T., & Steffen, V. J. (2009). Multiple surrogates: How cross-validation errors can help us to obtain the best predictor. *Structural Multidisciplinary Optimization*, 39(4), 439-457. <http://dx.doi.org/10.1007/s00158-008-0338-0>.
- Wangaard, F. F. (1950). *The Mechanical Properties of Wood*. New York, N.Y.: John Wiley and Sons.
- Whitney, J. D. (1999). Field test results with mechanical harvesting equipment in Florida oranges. *Appl. Eng. Agric.*, 15(3), 205-210. <http://dx.doi.org/10.13031/2013.5766>.
- Whitney, J. D., & Wheaton, T. A. (1984). Tree spacing affects citrus fruit distribution and yield. *Proc. Fla. State Hort. Soc.*, 97, 44-47.
- Wilson, T. R. (1932). Strength-moisture relations for wood. Tech. Bulletin 282. Washington, D.C.: USDA.
- Yung, C., & Fridley, R. B. (1975). Simulation of vibrations of whole tree system using finite elements. *Trans. ASAE*, 18(3), 475-481. <http://dx.doi.org/10.13031/2013.36613>.